Dilute $GaAs_{1-x}Bi_x$ Epilayers with different Bismuth Concentrations Grown by Molecular Beam Epitaxy: A Promising Candidate for Gamma Radiation Sensor Applications

Amra A. Alhassni [1,2,*], Jorlandio F. Felix[3, *], John Fredy R. Marroquin[3], Sultan Alhassan[4], Haifa Alghamdi[5], Amjad Almunyif [1,6], Walter M. de Azevedo[7], Juliana Lunz[8], Braulio S. Archanjo[8], Mohamed Henini[1]

[1]School of Physics and Astronomy, University of Nottingham, Nottingham NG7 2RD, UK
[2]Department of Physics, College of Science, Al-Baha University, 65779, Al-Makhwah, Saudi Arabia
[3]Institute of Physics, NFA: LAB-LINS, University of Brasília (UnB), Brasília, DF, 70910-900, Brazil
[4]Physics department, College of Science, Jouf University, P.O.Box: 2014, Sakaka, 42421, Saudi Arabia
[5]Physics department, College of Science, University of Jeddah, 21959, Saudi Arabia
[6]Department of Physics, College of Science, Princess Nourah bint Abdulrahman University (PNU), Riyadh, 11671, Saudi Arabia
[7]Departamento de Química Fundamental, Universidade Federal de Pernambuco (UFPE), CDU, 50740-560, Recife/PE, Brazil
[8]Materials Metrology Division, National Institute of Metrology, Quality and Technology, 25250-020 Duque de Caxias, Rio de Janeiro, Brazil;

[*]author contact: Jorlandio@unb.br; aalhasani@bu.edu.sa.

Abstract

Radiation interaction studies are very important for exploring the technological applications of new materials in radiation environments. This work reports the effect of gamma radiation dose on the structural and optical properties of dilute $GaAs_{1-x}Bi_x$ epitaxial layers grown with different Bismuth contents by MBE on conventional (100) GaAs substrates. The influence of radiation has been studied by X-Ray Diffraction (XRD), Raman spectroscopy, and photoluminescence (PL) measurements. The samples were also characterized by Scanning Transmission Electron Microscopy (STEM) and Scanning Electron Microscopy (SEM. Gamma radiation (γ-) was found to influence the optical properties of $GaAs_{1-x}Bi_x$ epitaxial layers. From Raman measurements it was found that the concentration of holes increased when the samples were irradiated. This result is in good agreement with photoluminescence results, which showed that the intensity of the main peak increases after irradiation, indicating that the optical properties have improved for all samples. Furthermore, the XRD data revealed that for irradiated $GaAs_{1-x}Bi_x$ samples, the crystallographic quality of the samples was slightly changed after irradiation. This result is consistent with the results of photoluminescence measurements, which demonstrated that the $GaAs_{1-x}Bi_x$ samples exposed to 50 kGy dose showed an increase in photoluminescence and full width at half maximum for all irradiated samples.

Keywords: dilute bismides, growth temperature, optical properties, defects, Gamma irradiation.

I. Introduction

Dilute III-V bismide semiconductors materials such as $GaAs_{1-x}Bi_x$ alloys display strong reduction in the band gap when only a small percentage of bismuth atoms is incorporated into the lattice of the host material like GaAs which has a band gap energy of 1.424 eV at 300 K. Particularly, a few percent of Bi incorporated into GaAs, i.e. $GaAs_{1-x}Bi_x$ with x being the Bi composition, leads to a giant bowing in the band gap energy (~ 88 meV/%Bi) [1], as well as an increase of the spin–orbit band splitting which helps reduce the non-radiative Auger recombination [2, 3]. In addition, the electron spin properties, which depend critically on the spin-orbit (SO) interaction, can be tuned in dilute bismides, making them suitable candidates for spintronic applications. It is important to note that the conduction band is barely affected by the Bi atoms. These remarkable properties such as reduction of the band gap make GaAsBi a suitable material for several device applications such as multi-junction solar cells [4], photonic devices [1], mid and near IR optoelectronic devices [5], THz (TeraHertz) emitters and detectors [6]. It is well known that the growth temperature of III-V alloys can significantly influence their crystalline quality. In fact, substitutional incorporation of Bi into the host lattice of III-V compounds requires low temperature growth. However, the growth of $GaAs_{1-x}Bi_x$ is more complicated than the growth of conventional III–V alloys. This is mainly due to the high tendency of Bi segregating to the surface during growth, which requires the growth temperature to be lowered to < 400 ℃ [7]. Low growth temperature of GaAs causes an increased density of defects as well as it leads to degradation of the optical quality of the alloys [7]. For instance, growing GaAs at temperatures lower than the optimal growth temperatures (~580–600 ℃) leads to the creation of many point defects, such as As-antisites (As_{Ga}), As-interstitials (As_i) and Ga vacancies [8, 9]. Electrical and optical properties of III-V semiconductor materials can be altered by intentionally incorporating impurities into the host lattice, and these may significantly influence the performance of electronic and optoelectronic devices. In general, defects can be created in semiconductor materials either intentionally or unintentionally through ionizing irradiation. Radiation induced defects can be divided into two types that are modified by ionizing irradiation: those created initially during growth of the crystal by substitution of a lattice atom with an impurity atom (extrinsic defect) and those created by atomic displacements of a standard lattice site element during irradiation (intrinsic defect). Ionizing radiation creates ions and free electrons, which in turn may be stabilized/trapped by radiation-induced defects before recombination can occur at normal lattice sites [10]. Gamma radiation is an indirectly ionizing and highly energetic electromagnetic radiation, which has a

large penetration power. In this sense, ionizing radiation, which can modify the optical and electrical properties of semiconductor materials, may lead to the development of new dosimeters and/or more efficient radiation detectors. Recent works show that there is a constant search to improve detectors/dosimeters by increasing sensitivity, offering measurements in real time and significantly reducing costs [11]. Thus, a deep understanding of the effect of gamma radiation on new materials is essential for the improvement of radiation sensors. Furthermore, due to radiation in space and the use of electronic devices in satellites, considerable amount of defects can be induced in semiconductors which, in turn, can cause degradation and decrease of the average lifetime of the devices [12]. Several groups have studied the effect of radiation treatment in metal/semiconductor Schottky diodes using a variety of radiation sources, including electron [13], neutron [14], swift heavy ions [15] and gamma radiation [16, 17]. However, the effects of gamma irradiation on $GaAs_{1-x}Bi_x$ thin films grown at different temperatures have not yet been investigated. Our findings show that radiation increased the quenching temperature of PL by more than 50 K for some of the samples. Specifically, we observed the most significant increase in the quenching temperature of PL, after radiation, in the sample with the highest Bi concentration. This behaviour indicates that radiation has a strong influence on the deep localized states within the bandgap of $GaAs_{1-x}Bi_x$. In this study, the influence of gamma irradiation dose on the structural and optical properties of $GaAs_{1-x}Bi_x$ samples grown by Molecular Beam Epitaxy (MBE) on (100) GaAs substrates is investigated in depth using a variety of methods such as Scanning Transmission Electron Microscopy (STEM), Scanning Electron Microscopy (SEM), X-Ray Diffraction (XRD), Raman spectroscopy, hole concentration and photoluminescence (PL) measurements.

II. Sample details

All $GaAs_{1-x}Bi_x$ film samples investigated in this work have been grown by solid-source MBE on semi-insulating (100) GaAs substrates under identical growth conditions to explore the effects of growth temperature, T_G, on the structural and optical properties of the irradiated samples as shown in **Error! Reference source not found.**~~Figure 1~~. For this purpose, a set of seven $GaAs_{1-x}Bi_x$ epilayers were grown at T_G= 300 ^{0}C, 310 ^{0}C, 320 ^{0}C, 325 ^{0}C, 340 ^{0}C, 345 ^{0}C and 365 ^{0}C and labelled as A, B, C, D, E, F and G, respectively. The samples were first heated to a temperature of 610 ^{0}C for 10 minutes to desorb the native oxide layer from the substrate surface. After that, an undoped GaAs buffer layer with a thickness of 400 nm was formed at a growth temperature of 580 ^{0}C and a growth rate of 1 monolayer per second. This was followed by a 20 min growth interruption during which the samples were cooled down to the appropriate

T_G and the growth rate lowered to ~0.1 monolayer per second. This was followed by the deposition of a 300 nm $GaAs_{1-x}Bi_x$ layer using a relatively large Bi flux twice that of As, while maintaining an approximately equal flux of As and Ga. This places the growth conditions well within the Bi saturation regime, where an alloying limit is imposed by the low miscibility of Bi into GaAs. More detailed information on the growth of $GaAs_{1-x}Bi_x$ is reported in Ref [18] .

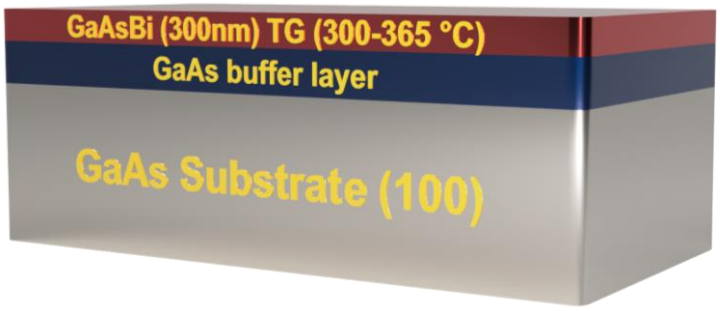

Figure 1: Schematic structure of a $GaAs_{1-x}Bi_x$ epilayers grown on semi-insulating (100) GaAs substrates at different growth temperatures.

It is important to note that the same piece of each sample mentioned above was measured before and after irradiation. The samples are labelled as NIR (non-irradiated) and IR (irradiated). The gamma radiation dose was 50 kGy. The optical characterization techniques used to investigate these samples are similar to NIR samples. The samples were then irradiated with a gamma cell Cobalt Irradiator (dose rate of 1.3 kGy/h) at dose of 50 kGy. PL spectra of all $GaAs_{1-x}Bi_x$ samples were investigated as a function of laser power and temperature using a Janis closed-loop helium cryostat. A green laser with a wavelength of 532 nm (2.33 eV) was used to excite the samples. Before subjecting the samples to gamma irradiation, each sample was evaluated using PL measurements to determine whether they were uniform. The PL signal was collected in a 0.5 m Andor monochromator fitted with an InGaAs detector. The Raman measurements were performed by employing a Horiba Lab RAM Evolution micro spectrometer at room temperature using a 532 nm laser line. The laser excitation powers of 5.35 mW and 0.107 mW, were used to obtain the correlation of Bi concentration with PL results and the hole concentration, respectively. In addition, SEM images and Transmission Electron Microscopy (TEM) lamellas were acquired using a Thermofisher Helios Nanolab 650. The images were made using a probe corrected Thermofisher Titan80-300 working at 200 keV. The images were collected using high-angle annular dark-field detector (HAADF) in STEM mode.

A. Microscopy

Figure 2~~Figure 2~~ shows the SEM images of the surfaces of all $GaAs_{1-x}Bi_x$ samples grown on (100) GaAs substrates at different growth temperatures. Droplets are clearly observed in the SEM images of the surfaces of $GaAs_{1-x}Bi_x$ samples as shown in Figure 2~~Figure 2~~.

Formatted: Font: Not Bold

Formatted: Font: Not Bold

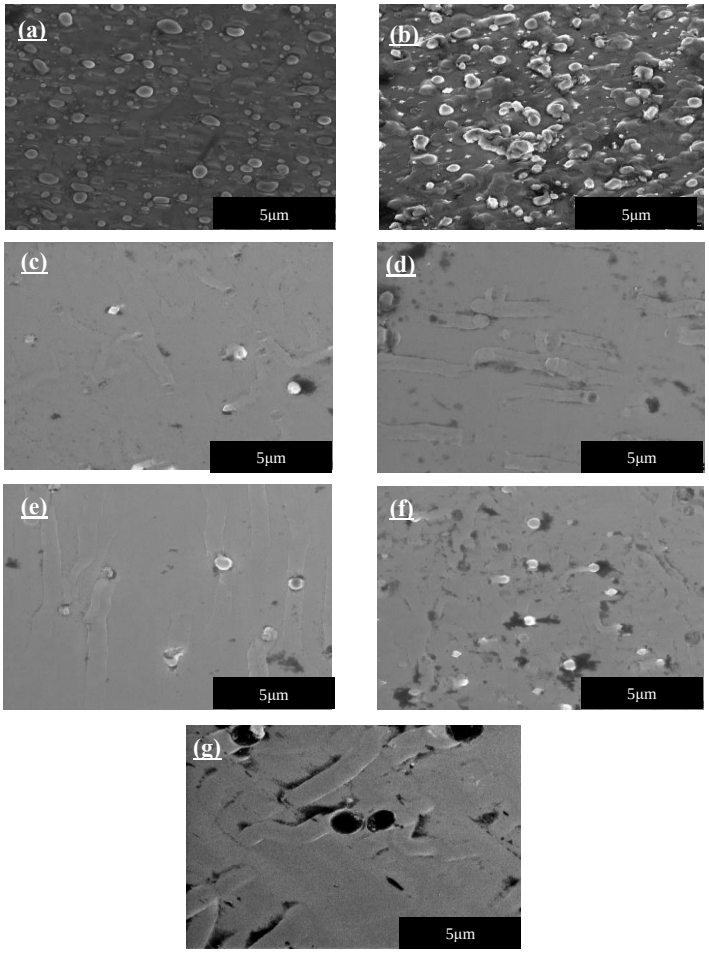

Figure 2: SEM images of the surfaces of $GaAs_{1-x}Bi_x$ samples grown on (100) GaAs substrates (a) sample A (T_G=300 ˚C), (b) sample B (T_G=310 ˚C), (c) sample C (T_G=320 ˚C), (d) sample D (T_G=325 ˚C), (e) sample E (T_G=340 ˚C), (f) sample F (T_G=345 ˚C), (g) sample G (T_G=365 ˚C).

The A (a) and B (b) samples exhibit many droplets, while samples C (c) to G (g) both droplets and self-aligned trailing nanotracks are present.

The growth mechanism of these droplets has been the object of study in many works [19, 20]. These Bi droplets, which are formed during the MBE growth of the $GaAs_{1-x}Bi_x$ epilayer, are in general associated with the non-uniformities of the thickness and composition of the growing layer. In fact, as expected, the samples with the highest surface concentrations of droplets are those with the lowest concentrations of Bi, as evidenced by SEM images shown in Figure 2~~Figures 2~~ (a), (b) and (g). This means that for these growth temperatures a lower concentration of Bi was incorporated into the GaAs host lattice. On the other hand, sample D, which was grown at 325 °C, has the highest concentration of bismuth (4.7%). As can be seen from Figure 2~~Figure 2~~ (d), this sample has the lowest number of both surface droplets and self-aligned trailing nanotracks. Especially for sample G, as shown in Figure 2~~Figure 2~~ (g), the self-aligned trailing tracks are wider with black drops at their ends, indicating that bismuth was not effectively incorporated into the GaAs host lattice. Interestingly, sample G grown at the highest temperature (365 °C) is amongst the samples that have also a low concentration of bismuth (2.8%), in agreement with the PL and Raman results which will be discussed in the following sections.

Formatted: Font: Not Bold, Font color: Black

Formatted: Font: Not Bold, Font color: Black

Formatted: Font: Not Bold, Font color: Black

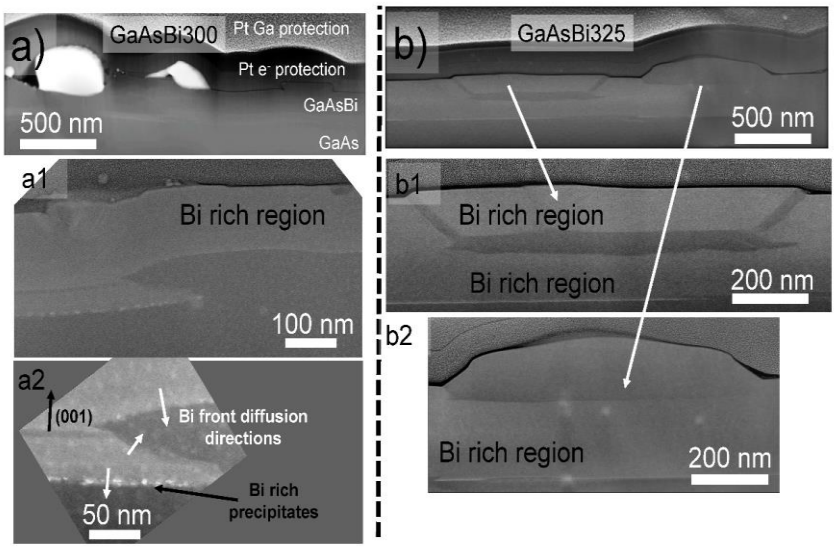

Figure 3: STEM images of (a) sample A (T_G=300 ˚C) and (b) Sample D (T_G=325 ˚C). From top to bottom one can see the Pt Ga and Pt e- protection layers deposited using Focused Ion Beam (FIB) and then the $GaAs_{1-x}Bi_x$ layer and finally the GaAs substrate. Details of the $GaAs_{1-x}Bi_x$ layer is shown in a1, a2, b1 and b2. The lamellas are oriented perpendicular to the droplets/nanotracks (see SEM images).

For the STEM analysis, the samples with lower and higher concentrations of Bi (sample A and D) were used as representative samples. STEM images, presented in Figure 3~~Figure 3~~a, show a large bismuth oxide precipitate, an inhomogeneous Bi distribution [19] along the film, and GaAs stripes having different sizes which are probably perpendicular sections of buried nanotracks [21]. The edges of the nanotracks have very specific angles as indicated in Figure 3~~Figure 3~~a2 by Bi diffusion front direction. Small Bi precipitates buried in the film are also shown in Figure 3~~Figure 3~~a2. The $GaAs_{1-x}Bi_x$ film in Sample D, see Figure 3~~Figure 3~~b, has a more homogenous Bi distribution than in Sample A, as can be also seen in the SEM images. In Figure 3~~Figure 3~~b1 buried GaAs nanotracks/droplets are observed, and interestingly they have two small extensions on both sides at specific angles which define a $GaAs_{1-x}Bi_x$ nanotrack as well. Figure 3~~Figure 3~~b2 shows the GaAs nanotrack region that is visible on the sample surface.

Formatted: Font: (Default) +Headings CS (Times New Roman), 12 pt, Not Bold, English (United States)

Formatted: Font: (Default) +Headings CS (Times New Roman), 12 pt, Not Bold, English (United States)

Formatted: Font: (Default) +Headings CS (Times New Roman), 12 pt, Not Bold, English (United States)

Formatted: Font: (Default) +Headings CS (Times New Roman), 12 pt, Not Bold, English (United States)

Formatted: Font: (Default) +Headings CS (Times New Roman), 12 pt, Not Bold, English (United States)

Formatted: Font: (Default) +Headings CS (Times New Roman), 12 pt, Not Bold, English (United States)

X-ray Diffraction (XRD)

Figure 4~~Figure 4~~ shows the XRD pattern for sample F (T_G=345 ^{0}C) with a Bi concentration of 4.3%. The XRD pattern shows three well defined peaks located at 31.63^0, 65.4^0 and 66.07^0 which are associated with the diffraction planes of (002) and (004) of $GaAs_{1-x}Bi_x$ and (004) of GaAs, respectively. The XRD pattern for IR sample grown at 345 ˚C indicates that its crystallographic behaviour was not considerably affected by irradiation, only a slight broadening of the peaks was observed. It is worth pointing out that similar results, not shown here, were obtained for samples grown at other temperatures. This is since radiation induces permanent defects, which are also observed by PL measurements, as will be discussed later. The inset on the right side of Figure 4~~Figure 4~~ shows a zoom of the $GaAs_{1-x}Bi_x$ (004) characteristic peak. A displacement of this peak (around 65.4º) as a function of the bismuth concentration/growth temperature was observed. It is important to point out the linear trend of $GaAs_{1-x}Bi_x$ (004) peak displacement as a function of Bi concentration, as can be seen in the inset on the left side of Figure 4~~Figure 4~~.

Formatted: Font: (Default) Times New Roman, 12 pt, Not Bold, Font color: Black, English (United States)

Formatted: Font: (Default) Times New Roman, 12 pt, Not Bold, Font color: Black, English (United States)

Formatted: Font: (Default) Times New Roman, 12 pt, Not Bold, Font color: Black, English (United States)

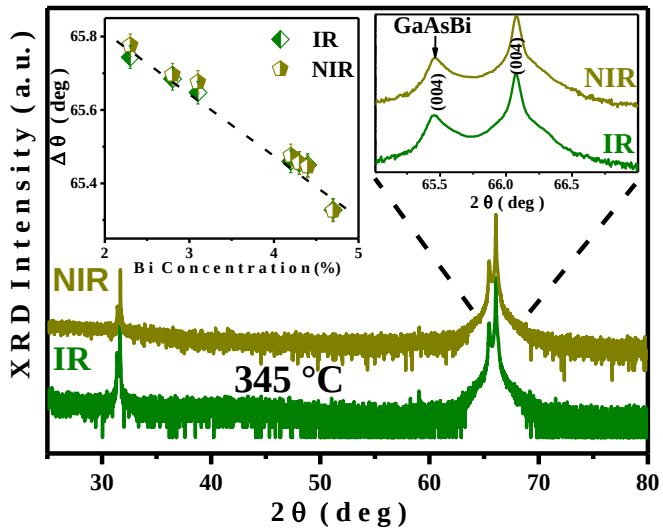

Figure 4: Diffraction pattern in the θ–2θ scan of X-ray diffraction measurements for sample F (T_G=345 ^{0}C) with Bi concentration x= 4.4%. The inset shows the diffraction pattern in the region between 2θ = 65.5° and 67º, where two peaks are associated with $GaAs_{1-x}Bi_x$ and GaAs. In the inset on the left side, a linear trend of $GaAs_{1-x}Bi_x$ (004) peak displacement as a function of Bi concentration is shown.

B. Raman Spectroscopy

Hall effect measurement is one of the most common methods used to determine the charge carriers' concentration in semiconductors, which is important for device fabrication. However, this technique requires the formation of Ohmic contacts which can alter the properties of the samples or even damage them. Alternatively, Raman spectroscopy is a versatile tool that can be used to determine the hole concentrations in $GaAs_{1-x}Bi_x$ samples without electrical contacts. In this sense, the hole concentration can be determined with a good accuracy using the relative intensities ratio of the unscreened longitudinal optical (ULO) phonon and the longitudinal optical phonon-hole-plasmon-coupled (LOPC) modes. Figure 5(a) shows the characteristic Raman spectra of $GaAs_{1-x}Bi_x$ at room temperature.

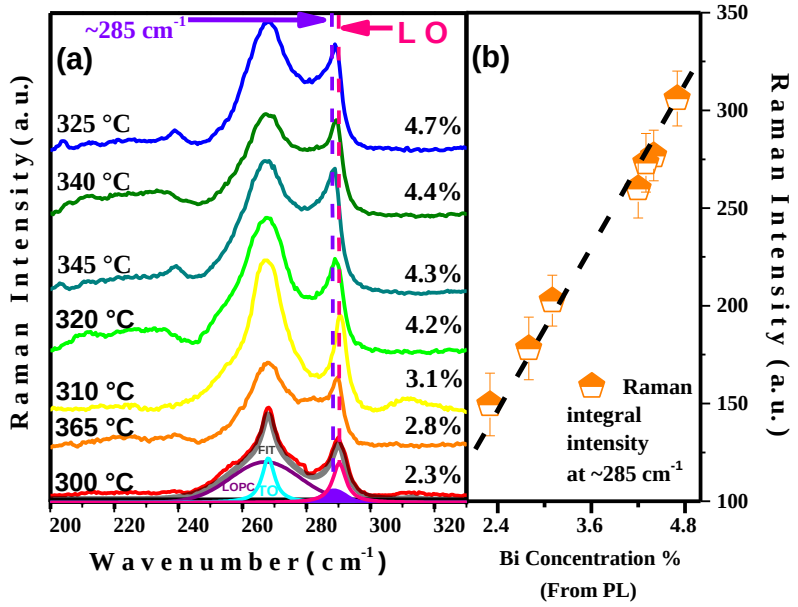

Figure 5: (a) Raman spectra from $GaAs_{1-x}Bi_x$ layers having with different Bi concentrations x. (b) Raman intensity from peak at ~285 cm^{-1} as function of Bi concentration showing a linear dependence.

The spectra display the Raman typical bands of GaAs in the range of 200-350 cm^{-1} [22]. The bottom of Figure 5~~Figure 5~~ shows the deconvolution using Lorentzian functions, which display the Raman bands associated with the transverse optical (TO) phonon and longitudinal optical (LO) phonon located at ~263 cm^{-1} and ~286 cm^{-1}, respectively [23]. In addition, a broader asymmetric band around 269 cm^{-1} due to the LOPC modes overlaps the TO phonon peak at ~267 cm^{-1}. Furthermore, a vibrational mode at ~285 cm^{-1} near the LO phonon peak is observed [22]. Previous studies showed that the Raman scattering signals from the LO and LOPC phonon follow the same Raman selection rules, indicating that the observed LOPC modes are also phonon-like [24]. Interestingly, as the content of Bi increases, first there is a slight redshift and then a blueshift of the LO phonon (for guide to the eyes, see the two vertical dashed lines in Figure 5~~Figure 5~~(a), which can be explained by the Bi-induced tensile and/or compressive stress [4]. Besides, as Bi concentration increases, the intensity of the phonon mode located at ~287 cm^{-1} becomes larger [22]. Figure 5~~Figure 5~~(b) also shows a very interesting

Formatted: Font: Not Bold

Formatted: Font: Not Bold

Formatted: Font: Not Bold

result, where Raman intensity of this mode exhibits a linear dependence as a function of the Bi concentration. This Raman band has been assigned to the disorder activated mode or a Fröhlich mode [25, 26]. In Figure 6~~Figure 6~~, the effects of gamma radiation on Raman spectra and hole concentrations of $GaAs_{1-x}Bi_x$ samples irradiated with a 50 kGy dose are presented. It will be also shown that Raman spectroscopy has proved to be a versatile tool for studying defects in $GaAs_{1-x}Bi_x$ samples. It is important to point out that low laser excitation powers were used to perform all Raman measurements. This procedure was adopted because high laser excitation powers may give incorrect hole concentration values [22]. Sixin et al. showed that laser powers lower than 0.4 mW provides results compatible with other techniques. According to this, in Figure 6~~Figures 6~~(a) and (b) are shown Raman spectra that were obtained using 0.107 mW as the excitation power for the IR and NIR GaAsBi samples. When carefully comparing the spectra, subtle differences are observed which are evident in the analysis below. First, to obtain the hole concentration from Raman spectroscopy, it is necessary to relate the relative intensities of the LO and LOPC phonon modes using the followings equation [23, 24].

$$p = \frac{8\varepsilon_0\varepsilon_s\alpha^2\phi_B}{e\left[ln\left(1+\frac{\zeta_A}{\zeta_S}\right)\right]} \qquad (1)$$

where ε_0 is the vacuum permittivity, ε_s is the static dielectric constant, α is the absorption coefficient and ϕ_B is the surface potential barrier [27]. Since the values of α, ε_s and ϕ_B for GaAsBi are not available, those of GaAs were used, $\varepsilon_s = 12.8$, $\phi_B = 0.5$ eVand $\alpha \approx 231 \times 10^3$ cm^{-1}, for the excitation wavelength of 532 nm [23, 28, 29]. $\zeta_A = A_{LO}/A_{LOPC}$ is the ratio of the integrated intensity of ULO mode and LOPC mode in the Raman spectrum. $\zeta_S = I_{LO}/I_{LOPC}$ is the relative Raman scattering efficiencies of the pure LO phonons and the coupled mode in a volume element. By comparing the efficiencies of the modes I_{LO} and I_{LOPC} at different excitation energies, one can obtain ζ_S =2 [22, 23].

Figure 6~~Figure 6~~(c) shows the hole concentrations as a function of bismuth concentration of the NIR samples (black stars) and IR samples (red balls). Note that initially the hole concentration in NIR samples increases proportionally until reaching 4.2% of bismuth, then decreases and finally increases again. It is very important to note from Figure 6~~Figure 6~~(c), that the concentration of holes increased for all samples after radiation. Furthermore, the hole concentrations of the IR samples show a similar behaviour, i.e. increase/decrease/increase, but

Formatted: Font: Not Bold, English (United Kingdom)

Formatted: Font: (Default) +Headings CS (Times New Roman), Not Bold

Formatted: Font: Not Bold

Formatted: Font: Not Bold

with a more pronounced trend than the one displayed by the NIR samples. These findings show that these results are consistent with the PL results that will be discussed later, since all samples showed an increase in PL intensity after irradiation. As is well known, a considerable deformation of the GaAs lattice occurs due the large size of bismuth atoms, which causes an increase in the carrier-phonon coupling. Associated with this, the incorporation of Bi into GaAs host lattice also produces a strong effect on the carrier recombination process due to an increase in the density of localized states [30, 31]. Compressive strain is also commonly observed in GaAs due to bismuth incorporation [30]. These effects caused in the crystal lattice of GaAs due to the incorporation of Bi causes disorder and/or residual strains which alter the frequencies of phonons and their lifetime, and can be identified by means of Raman spectroscopy [32]. In fact, the GaAs LO Raman mode frequency shifts are deeply related to the compressive and tensile strains, resulting in positive and negative frequency shifts, respectively [33, 34]. In Figure 6~~Figure 6~~(d) are plotted the Raman shift of LO mode from the NIR (black squares) and IR (solid red circles) samples. As can be seen in Figure 6~~Figure 6~~(d), an evident frequency shift of the LO mode is observed as a function of Bi concentration. Interestingly, when comparing NIR and IR samples, a positive or negative frequency shifts in LO mode maybe observed depending on the concentration of Bi. Remarkably, the samples that showed a negative change in the frequency of the LO mode were those that showed the smallest increase in the PL signal after radiation (to be discussed later). This suggests that these samples showed tensile strains after irradiation. On the other hand, samples with Bi concentrations of 4.3% and 4.4% showed a positive frequency shift of the LO mode after irradiation, indicating that the irradiation caused a compressive strain. More interesting, as will be shown below, sample F with 4.3% of Bi showed the highest increase in the PL signal after irradiation.

Formatted: Font: Not Bold

Formatted: Font: Not Bold

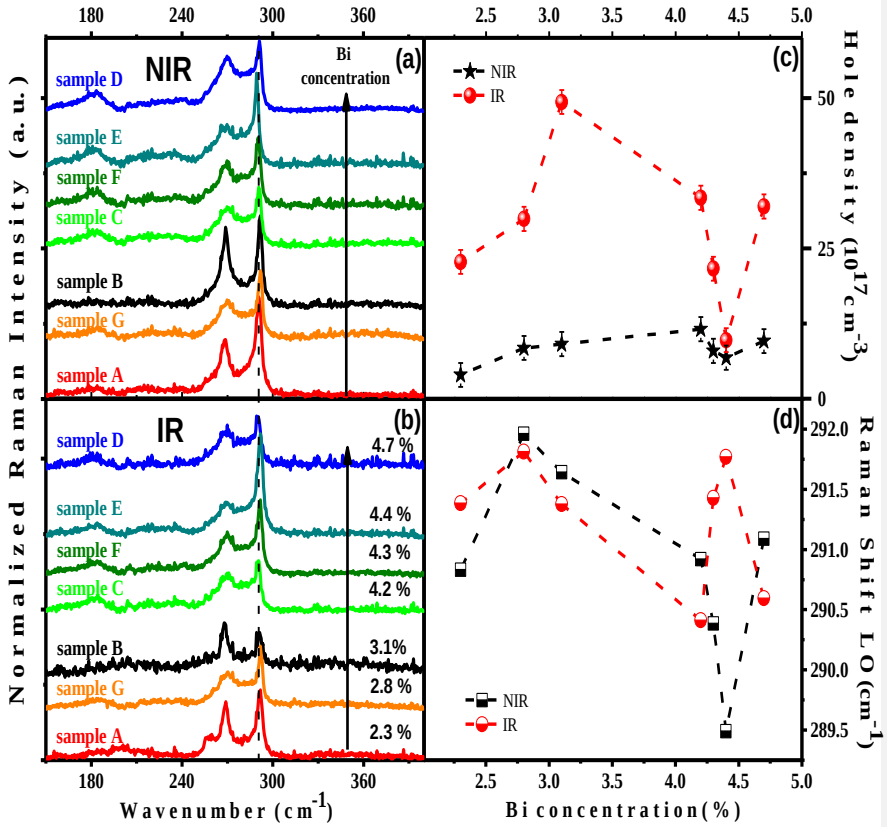

Figure 6: Raman spectra from $GaAs_{1-x}Bi_x$ samples having different Bi concentrations x. The measurements were performed using 0.107 mW as the excitation power (a) non-irradiated (NIR) samples and (b) Irradiated (IR) samples. (c) The hole concentration (calculated from equation 1) versus Bi content for IR and NIR samples. (d) Raman shifts of LO mode versus Bi content for the NIR and IR samples.

C. Photoluminescence

This section will report on the optical properties of $GaAs_{1-x}Bi_x$ thin films grown on the conventional (100) GaAs substrates at different growth substrate temperatures, namely A, B, C, D, E, F and G. The effects of growth temperature on the optical properties of $GaAs_{1-x}Bi_x$ layers were investigated by photoluminescence spectroscopy measurements at various temperatures and excitation powers. PL measurements were performed using a green laser (532

nm) with pump powers ranging from 0.5 mW to 65 mW. Figure 7~~Figure 7~~ shows the PL spectra at low temperature of 10 K for all NIR $GaAs_{1-x}Bi_x$ samples grown on (100) GaAs substrates at different growth temperatures and at a laser excitation power P_{EXC} = 16 mW (0.91 W/cm^2). Overall, the PL peaks at 1.30 eV, 1.23 eV 1.14 eV, 1.09 eV, 1.12 eV, 1.13 eV and 1.26 eV are related to GaAsBi samples A, B, C, D, E, F and G. respectively. For sample A, the PL emission energy found at 1.3 eV is related to $GaAs_{1-x}Bi_x$ and the peaks between 1.34 eV and 1.4 eV could be due to some defects. It is worth noting that the $GaAs_{1-x}Bi_x$ PL emission of sample A (T_G=300 $^{\circ}$C) is the weakest and the broadest amongst all samples. A small increase of 10 $^{\circ}$C in the growth temperature from 300 $^{\circ}$C (sample A) to 310 $^{\circ}$C (sample B) improved the PL intensity of sample B by 2.6 times as compared to sample A. However, a large enhancement by a factor of 5.6 in the $GaAs_{1-x}Bi_x$ PL intensity was observed by further increasing the growth temperature above 310 $^{\circ}$C. These PL results could be explained by the competition mechanisms that generate and reduce structural defects. For example, when the growth temperature is lower than the optimal GaAs growth temperature (T_G = 400-630 °C), native defects which are attributed to nonradiative energy states such as Ga vacancies and As antisites are typically created in the material [35, 36]. On the other hand, Lu et al reported [37] that at the low growth temperatures required to incorporate a small amount of Bi ($x < 0.045$) during GaAs growth, Bi atoms induce localized states close to the maximum of the valence band (MVB) because of Bi-pair and Bi-cluster formation. These localized states behave as trapping centres for bound holes, which can recombine radiatively. At the same time, Bi can behave as a surfactant, which enhances the quality of the material by decreasing the defects because of the low growth temperature used [38]. One mechanism decreases the carrier loss by nonradiative centres for samples A and B (when $T_G \leq 310$ $^{\circ}$C), and the other mechanisms improve the efficiency of the PL (when $T_G \geq$ 320 $^{\circ}$C) for samples C, D, E, F and G. In this work, sample A which was grown at the lowest growth temperature of 300 $^{\circ}$C has higher density of defects than the other samples as evidenced by the lower PL intensity. These results are consistent with SEM data which demonstrated that sample A (T_G =300 $^{\circ}$C) has the highest surface concentration of droplets and the lowest concentration of Bi, meaning that for these low growth temperatures a lower concentration of Bi was incorporated into the GaAs host lattice. On the other hand, the optimum growth temperature for maximum Bi incorporation (4.7%) was found to be 325 ^{0}C (sample D) which is in good agreement with SEM data which showed that this sample has a lower number of both surface droplets and self-aligned trailing nanotracks. Furthermore, the PL spectra exhibit two different behaviours depending on the growth temperatures: (i) a red shift of 21 meV of the PL peak from 1.3 eV (T_G =300 ^{0}C) to 1.09 eV (T_G =325 ^{0}C) was observed when the growth

Formatted: Font: (Default) Times New Roman, 12 pt, Not Bold, Font color: Black

temperature was increased (ii) a blue shift of 17 meV of the PL peak from 1.09 eV (T_G =325 °C) to 1.26 eV (T_G =365 °C) was noted as the growth temperature increased. These findings are in good agreement with Raman results which showed that as the content of Bi increases, first there is a slight redshift and then a blueshift of the LO phonon, which can be explained by the Bi-induced tensile and/or compressive stress [4]. The PL spectra shown in the Figures below (7, 8(a) and (b)) are presented using a linear scale divided by 1000 in the intensity axis in order to evidence different effects.

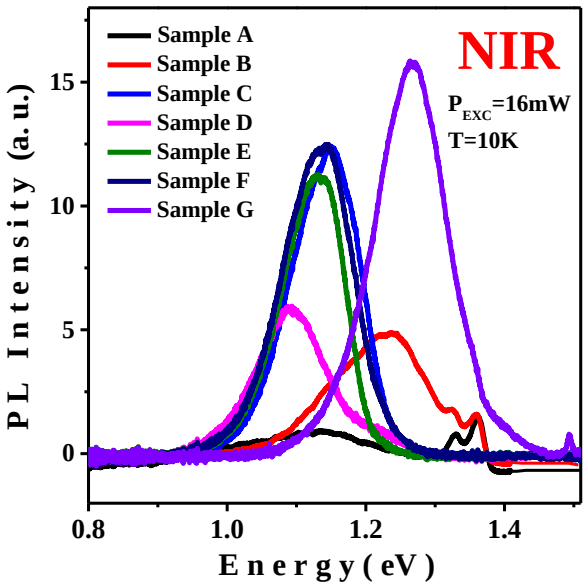

Figure 7: 10 K PL spectra of the $GaAs_{1-x}Bi_x$ epilayers grown on (100) GaAs substrates for samples A, B, C, D, E, F and G, using a green laser (532 nm) with P_{EXC}= 16 mW.

To verify the effect of ionizing radiation on optical properties of $GaAs_{1-x}Bi_x$ samples, power dependent PL measurements were carried out. Figure 8 (a) displays the PL spectra at 10 K for sample F (345 °C), namely non-irradiated and irradiated with a dose of 50 kGys using a laser excitation power of 16 mW (0.91 W/cm^2).The effects of gamma radiation on $GaAs_{1-x}Bi_x$ films is clearly demonstrated in Figures 8 (a), (b) and (c) by the following observations: (i) no blue shift of the $GaAs_{1-x}Bi_x$ film PL peak emission energy was observed (see Figure 8 (a) and (b)), (ii) there are enhancements of the PL intensities by a factor of 1.06, 1.2, 1.9, 1.4, 1.3, 2.4 and

1.1 for all samples A, B, C, D, E, F and G, respectively (see Figure 8 b). The latter observation supports the Raman hole concentration results which demonstrated an increase in the carrier concentration for all IR $GaAs_{1-x}Bi_x$ samples at 50 kGy dose in comparison with the NIR samples, (iii) The values of the PL FWHM (full width at half maximum) of the IR samples are higher than those of the NIR samples as shown in Figure 8 (c). This finding demonstrates that IR samples, in terms of defects, have worse quality compared to NIR samples, i.e., as expected, the defect number increased after radiation. As can be seen in Figure 8 (b), there is also an increase in the PL intensity of all samples, however, this enhancement is largest for the sample with a Bi concentration of 4.3% (sample F). These PL results are also in good agreement with the Raman results, which showed a positive frequency shift of the LO mode after irradiation. This shift in frequency after irradiation indicates that the irradiation caused a compressive strain in the material. However, the samples with a lower Bi concentration showed a smaller increase in the PL signal after being exposed to radiation. These samples had a Bi concentration of 2.3% (sample A), 2.8% (sample G), and 3.1% (sample B). These results are consistent with the findings obtained from the Raman measurements, which demonstrated a decrease in the frequency of the LO mode. After being exposed to ionising radiation, these above samples demonstrated signs of tensile strain. In addition, these results are also in good agreement with SEM and STEM data, which showed that the samples with the highest surface concentrations of droplets are those with the lowest concentrations of Bi (see SEM images illustrated in Figures 2(a), (b) and (g)). This indicates that for these growth temperatures a lower concentration of Bi was incorporated into the GaAs host lattice. A very interesting result is that the PL intensity of all IR samples quenches at higher temperatures than those of the NIR samples (results not shown here).

During the interaction of gamma-ray photons with a semiconductor material, several processes can occur. Gamma-rays can be considered as a type of indirect ionizing radiation, which can transfer their energy involving a two-stage process. In the first stage, the photons lose some of their kinetic energy in collisions with secondary charged particles present in the semiconductor through which the radiation passes, and in the second stage, these secondary charged particles lose their energy either through collisions or through radiation emission (e.g., Bremsstrahlung radiation) [10].This process can release charges (electrons, free radicals) which are trapped at defects in the crystal lattice of a semiconductor material. In our specific case, the substantial difference in atomic size between Bi and As leads to several fascinating optical and structural characteristics in $GaAs_{1-x}Bi_x$ (in this alloy Bi substitutes As). Furthermore, Bi acts as an

isovalent impurity in GaAs, causing a substantial perturbation in the valence band structure [39]. The process of ionization can be comprehended by analysing the relationship between the mass attenuation coefficient (μ) and the reaction cross-section σ (cm^2), i.e, $\mu = N_0\sigma/A$, where N_0 is Avogadro's number (6.02×10^{23}) and A is the atomic weight of the absorber [40] . The atomic weight of Bi, Ga and As are A^{Bi} = 208.9804 u, A^{As} = 74.9216 u and A^{Ga} = 69.723 u, respectively, where u is the atomic mass unit. By considering the cross-section only, it is clear that the cross section of Bi is around three times higher than that of As and Ga (A^{Bi}/A^{As}~2.8 and A^{Bi}/A^{Ga} ~ 3.0). C. Weiss and colleagues conducted a study on the influence of electron and proton irradiation on the minority carrier lifetime of p-type Ge wafers[41]. According to their investigation, the displacement of a single Ge atom from its lattice position results in the creation of a vacancy and an interstitial atom, also known as a Frenkel pair, occurs on average when exposed to MeV electrons or photons. These defects have the potential to act as recombination centers for electron-hole pairs. The generation of Frenkel pairs in solids is a well-established phenomenon when exposed to ionizing radiation. The formation of these pairs exhibits an energy threshold that is related to the atomic weight.~~:~~ For example, ~~–~~heavier elements such as Bi have a higher threshold, while lighter elements like As and Ga have a lower threshold. Additionally, the effective cross-section for pair creation on different sublattices in materials containing these elements is dependent on the energy of the ionizing radiation. In our study, as the photon energy lines are 1.17 MeV and 1.32 MeV, i.e., the radiation energy is below of the Bi threshold (~1.2 MeV) [42] and the creation of Frenkel pairs will be mostly on As or Gas sublattices [42]. On this basis, our results suggest that the ionization effect on bismuth is lower when compared to Ga and As atoms in $GaAs_{1-x}Bi_x$ films. Therefore, the results indicate that samples with lower concentrations of bismuth, there was a relatively modest enhancement in the PL signal, whereas at high concentrations, a significant increase in the PL signal was observed. This observation suggests that, at this irradiation energy, Bi atoms within the sublattice becomes resistant to irradiation, potentially acting as a form of post-radiation lattice compensation~~ post radiation~~. Finally, heating due to ionizing radiation could also be considered as another possible contribution to the increase in the PL signal of the samples [43] Gamma radiation can cause a temperature increase which induces structural changes in the $GaAs_{1-x}Bi_x$ alloy. In this case, gamma radiation could cause a kind of thermal annealing, inducing a process of activation of dopants, consequently, contributing to the increase of the PL signal.

Commented [MH(1]: Check this Jorlandio

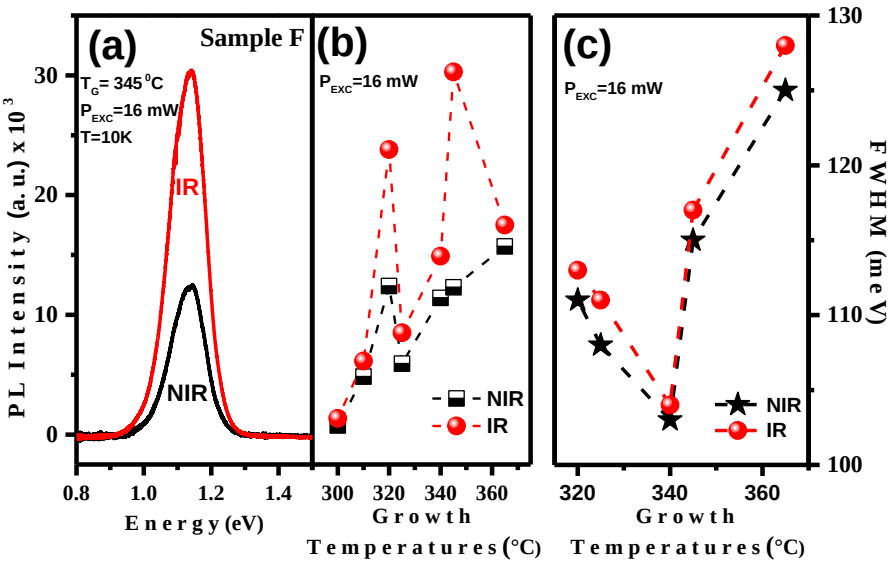

Figure 8: (a) 10 K PL spectra of $GaAs_{1-x}Bi_x$ epilayers grown on (100) GaAs substrates for sample F (345 ^{0}C) (NIR and IR with 50kGy dose). (b) PL peak intensity and (c) PL FWHM of NIR and IR $GaAs_{1-x}Bi_x$ samples as function of growth temperature. The measurements were carried out using a green laser (532 nm) and P_{EXC}= 16 mW.

Furthermore, sample E (T_G = 340 ^{0}C) with Bi concentration of 4.4% has the lowest FWHM before and after exposure to 50 kGy dose of gamma radiation, indicating a higher Bi uniformity and better optical properties of the thin film. However, sample G (T_G = 365 $^\circ$C) with Bi concentration of 2.8 % has the highest FWHM before and after exposure to 50 kGy dose of gamma radiation. This finding is consistent with the SEM and STEM results (illustrated in Figure 2~~Figure 2~~ (g)) which demonstrated that the self-aligned trailing tracks are wider with black drops at their ends, indicating that bismuth was not effectively incorporated into the GaAs host lattice. The presence of Bi clusters will be shown by analysing the temperature dependence of PL intensity with a modified Arrhenius equation [30, 44, 45]:

Formatted: Font: Not Bold

$$I(T) = I(0)/[1 + A_1 \exp\left(-{}^{E_1}/_{k_B T}\right) + A_2 \exp\left(-{}^{E_2}/_{k_B T}\right)] \quad (2)$$

where I(T) and I(0) are the PL integrated intensity at temperature T and 0 K, respectively. E_1 and E_2 are the thermal activation energies, A_1 and A_2 are the non-radiative and radiative recombination probabilities, k_B is the Boltzmann constant. Figure 9~~Figure 9~~ shows a plot of integrated PL intensity (IPL) versus 1/ k_BT. The activation energies were obtained from Arrhenius fitting for both NIR and IR samples.

Formatted: Font: (Default) Times New Roman, 12 pt, Not Bold

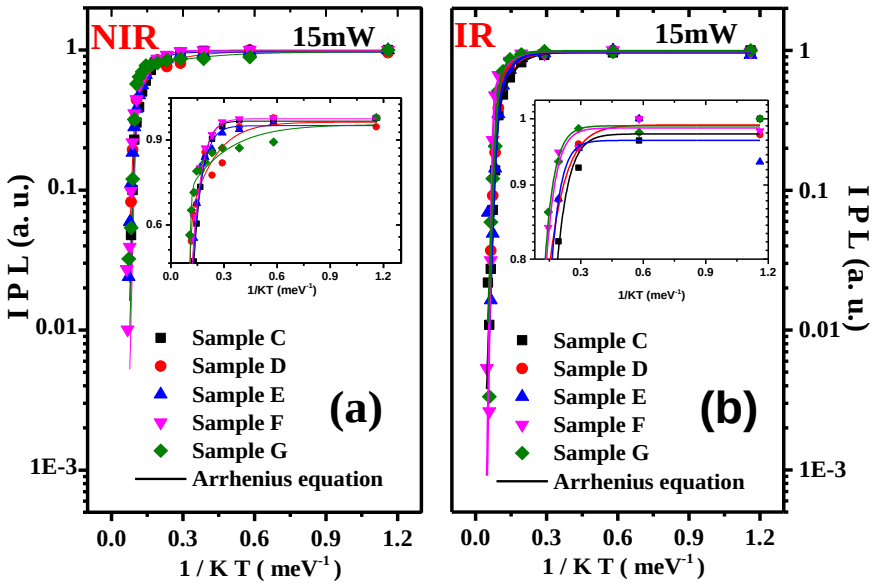

Figure 9: Arrhenius plots of integrated PL intensity (IPL) of $GaAs_{1-x}Bi_x$ epilayers grown on (100) GaAs substrates for samples C, D, E, F and G (a) NIR samples; (b) IR samples. Solid lines illustrate the fit to the experimental data using equation 2. The inserts show zoomed areas of the plots.

Table I summarises the E_1 and E_2 values for all samples. The activation energies obtained for all samples indicate the formation of Bi clusters and alloy disorder [46]. Indeed, the lower activation energy value (E_1) has been related to Bi cluster and Bi pair formation, while the higher activation energy value (E_2) has been related to the $GaAs_{1-x}Bi_x$ alloy disorder [47]. A recent study [30] found very similar behaviour in $GaAs_{1-x}Bi_x$ samples. All IR samples have larger E_1 activation energies for the low temperature regimes than the NIR samples, except for sample C (T_G =320 ^{0}C). In contrast, in the high temperature regimes all NIR samples have larger E_2 activation energies than the IR samples, except for sample F (T_G =345 ^{0}C). It is important to note that the highest E_2 activation energies are found to be in sample F (T_G =345

°C), before and after being exposed to gamma radiation at 175.8 meV and 250.7 meV, respectively. This sample with Bi concentrations of 4.3 % showed a positive frequency shift of the LO mode after irradiation, indicating that the irradiation caused a compressive strain. More interesting is that sample F showed the highest increase in the PL signal after irradiation. Finally, these findings not only indicate and contribute to a better understanding of defects in $GaAs_{1-x}Bi_x$, but also demonstrate that these materials can be used as efficient and highly sensitive ionising radiation detectors. More interestingly, the detection of ionizing radiation could be monitored by optical measurements, demonstrating the versatility of this material system.

Table I. Arrhenius fitting parameters for NIR and IR samples.

Samples	GaAsBi Samples grown at T_G (°C)	Activation energy (meV)			
		$E_{1(NIR)}$	$E_{2(NIR)}$	$E_{1(IR)}$	$E_{2(IR)}$
C	320	25.8	194.9	19.4	123.7
D	325	8.2	118.8	13.5	105.4
E	340	22.1	125.9	23.9	122.9
F	345	21.5	175.8	23.2	250.7
G	365	4.9	164.7	23.3	116.7

The incorporation of Bi into GaAs causes a significant reduction of its bandgap energy. This phenomenon is commonly explained by the valence-band anti-crossing model, which suggests that the interaction between the valence band of GaAs and resonant localized Bi states is responsible for it. Conversely, the presence of disorder effects, such as potential fluctuations attributed to the Bi content and the existence of Bi clusters within the alloy structure, contributes to an increase in the density of localized states. In addition to other effects, this disorder results in a significant reduction of the PL intensity (causing PL thermal quenching at relatively low temperatures) as the temperature increases, primarily due to the enhanced nonradiative recombination of thermally delocalized carriers in $GaAs_{1-x}Bi_x$ samples [45].

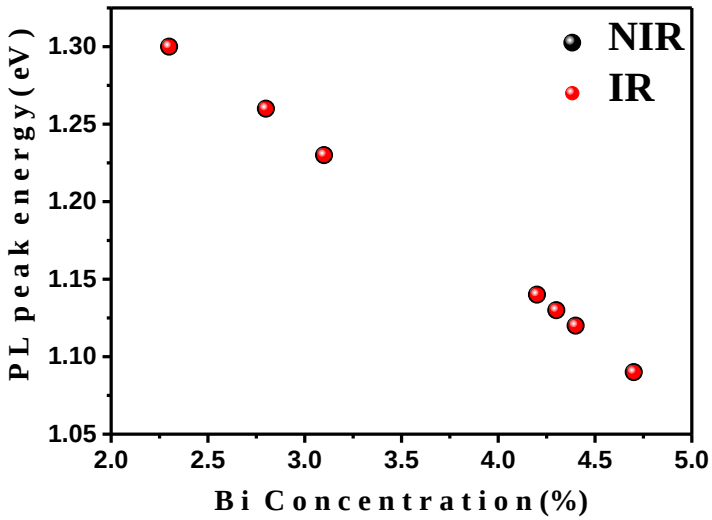

Figure 10: 10 K PL peak energy of $GaAs_{1-x}Bi_x$ epilayers grown on (100) GaAs substrates for samples A, B, C, D, E, F and G: for NIR and (b) IR with 50kGy dose. The measurements were carried out using a green laser (532 nm) and P_{EXC}= 16mW.

Fascinatingly, we observed a quenching of the PL signal in the irradiated samples C, D, E, F, and G at temperatures of 240 K, 220 K, 220 K, 240 K, and 220 K, respectively (not shown here). Notably, we found that the PL signal of the non-irradiated samples quenched at lower temperatures, namely 200 K, 170 K, 190 K, 200 K, and 190 K for samples C, D, E, F, and G, respectively. This suggests that radiation increased the temperature range over which the PL signal can be detected by more than 50 K for some of the samples. Specifically, we observed the most significant increase in the quenching temperature of PL, after radiation, in the sample with the highest Bi concentration. Another interesting observation is that the position of the PL peak remains unchanged upon exposure to radiation, (not shown here). This suggests that radiation did not affect the band structure of $GaAs_{1-x}Bi_x$ semiconductor alloys. However, much more research needs to be done to better understand the effect of radiation on $GaAs_{1-x}Bi_x$ alloys. Our results indicate that radiation had a strong influence on the density of localized states. Shakfa et al. [45] suggested that the PL intensity provides a clue for the presence of deep localized states within the bandgap of $GaAs_{1-x}Bi_x$. However, they also stated that additional research is required to confirm and characterize these states. We believe that radiation

significantly impacts these deep localized states. Finally, since the XRD, Raman and PL results did not indicate structural changes in $GaAs_{1-x}Bi_x$ samples after radiation, it is suggested that the main related effect is a process of passivation of deep localized states. However, further studies will be necessary in order to verify the effect of ionizing radiation on deep localized states.

IV. Conclusion

The effects of gamma radiation on the structural and optical properties of $GaAs_{1-x}Bi_x$ epilayers grown on (100) GaAs substrates by MBE with different Bismuth Concentrations were investigated by using STEM, SEM, XRD, Raman and PL techniques. The PL measurements showed that samples which were subjected to a dose of gamma rays of 50 kGy showed enhanced PL intensity in comparison to other samples which had not been irradiated. This result is consistent with Raman measurements which demonstrated that the concentration of holes increased in all IR samples as compared to NIR samples. The temperature dependence of the PL FWHM spectra in the range 10 K - 240 K was also studied. It was found that the NIR samples have the lowest FWHM compared to IR samples. The XRD results for IR samples indicated that the crystallographic behaviour of the samples was not considerably affected by irradiation. Additionally, the sample with Bi concentration of 4.4% (T_G = 340 ^{0}C) has the lowest FWHM before and after exposure to 50 kGy dose of gamma radiation, indicating a higher Bi uniformity and better optical properties of the thin films. The STEM and SEM results showed that the self-aligned trailing tracks are wider and have black drops at their ends, indicating that bismuth was not effectively incorporated into the GaAs host lattice. Nevertheless, the sample with lowest Bi concentration has the highest FWHM before and after gamma radiation exposure of 50 kGy. Our study highlights an important finding: GaAsBi-based devices with a bismuth concentration ranging from 2.3% to 4.7% exhibit remarkable resistance to radiation doses lower than 50 kGys, with no significant impact on their structural integrity. This result has significant implications for the development of next-generation devices such as multi-junction solar cells, photonic devices, and long-wavelength optoelectronic devices, which could be utilized in moderate irradiation environments. Additionally, the present research makes valuable contributions to the fundamental understanding that could be helpful for potential future applications of $GaAs_{1-x}Bi_x$ bulk alloys, specifically regarding the impact of ionizing radiation at varying levels of bismuth doping.

Acknowledgements

The author would like to express her gratitude to Al-Baha University, Saudi Arabia, for providing her with a PhD scholarship. Jorlandio F. Felix acknowledges CNPq and Fundação de Apoio à Pesquisa do Distrito Federal (FAPDF) for financial support (193.00001823/2022-10).

REFERENCES

[1] S. Francoeur, M.-J. Seong, A. Mascarenhas, S. Tixier, M. Adamcyk, T. Tiedje, Band gap of GaAs 1− x Bi x, 0< x< 3.6%, Applied physics letters, 82, (2003), 3874-3876.
[2] Z. Batool, K. Hild, T. Hosea, X. Lu, T. Tiedje, S. Sweeney, The electronic band structure of GaBiAs/GaAs layers: Influence of strain and band anti-crossing, Journal of Applied Physics, 111, (2012), 113108.
[3] B. Fluegel, S. Francoeur, A. Mascarenhas, S. Tixier, E. Young, T. Tiedje, Giant spin-orbit bowing in GaAs 1− x Bi x, Physical review letters, 97, (2006), 067205.
[4] Z. Zhou, D.F. Mendes, R.D. Richards, F. Bastiman, J.P. David, Absorption properties of GaAsBi based p–i–n heterojunction diodes, Semiconductor Science and Technology, 30, (2015), 094004.
[5] V. Pačebutas, K. Bertulis, A. Bičiūnas, A. Krotkus, Low-temperature MBE-grown GaBiAs layers for terahertz optoelectronic applications, physica status solidi c, 6, (2009), 2649-2651.
[6] K.K. Nagaraja, Y.A. Mityagin, M.P. Telenkov, I.P. Kazakov, GaAs (1-x) Bi x: a promising material for optoelectronics applications, Critical Reviews in Solid State and Materials Sciences, 42, (2017), 239-265.
[7] X. Lu, D. Beaton, R. Lewis, T. Tiedje, M. Whitwick, Effect of molecular beam epitaxy growth conditions on the Bi content of GaAs 1− x Bi x, Applied Physics Letters, 92, (2008), 192110.
[8] Ł. Gelczuk, J. Kopaczek, T.B. Rockett, R.D. Richards, R. Kudrawiec, Deep-level defects in n-type GaAsBi alloys grown by molecular beam epitaxy at low temperature and their influence on optical properties, Scientific Reports, 7, (2017), 12824.
[9] A. Mohmad, F. Bastiman, C. Hunter, J. Ng, S. Sweeney, J. David, The effect of Bi composition to the optical quality of GaAs1− xBix, Applied Physics Letters, 99, (2011), 042107.
[10] G. Halverson, Marine isotope stratigraphy, in: Encyclopedia of Scientific Dating Methods, Springer, (2013).
[11] H. Alehdaghi, E. Assar, B. Azadegan, J. Baedi, A.A. Mowlavi, Investigation of optical and structural properties of aqueous CdS quantum dots under gamma irradiation, Radiation Physics and Chemistry, 166, (2020), 108476.
[12] G.A. Umana-Membreno, J. Dell, G. Parish, B. Nener, L. Faraone, U. Mishra, /sup 60/Co gamma irradiation effects on n-GaN Schottky diodes, IEEE Transactions on Electron Devices, 50, (2003), 2326-2334.
[13] S. Krishnan, G. Sanjeev, M. Pattabi, Electron irradiation effects on the Schottky diode characteristics of p-Si, Nuclear Instruments and Methods in Physics Research Section B: Beam Interactions with Materials and Atoms, 266, (2008), 621-624.
[14] L. Zhang, Y. Zhang, Y. Zhang, C. Han, Neutron radiation effect on 4H-SiC MESFETs and SBDs, Journal of Semiconductors, 31, (2010), 114006.
[15] A.T. Sharma, S. Kumar, Y.S. Katharria, D. Kanjilal, Effects of swift heavy ion irradiation on the electrical characteristics of Au/n-GaAs Schottky diodes, Applied surface science, 254, (2007), 459-463.

[16] N. Al Saqri, J. Felix, M. Aziz, D. Jameel, C. De Araujo, H. Albalawi, F. Al Mashary, H. Alghamdi, D. Taylor, M. Henini, Investigation of the effects of gamma radiation on the electrical properties of dilute GaAs1− xNx layers grown by Molecular Beam Epitaxy, Current Applied Physics, 15, (2015), 1230-1237.
[17] Ş. Karataş, A. Türüt, Ş. Altındal, Effects of 60Co γ-ray irradiation on the electrical characteristics of Au/n-GaAs (MS) structures, Nuclear Instruments and Methods in Physics Research Section A: Accelerators, Spectrometers, Detectors and Associated Equipment, 555, (2005), 260-265.
[18] J. Steele, J. Horvat, R.A. Lewis, M. Henini, D. Fan, Y.I. Mazur, V. Dorogan, P. Grant, S.-Q. Yu, G. Salamo, Mechanism of periodic height variations along self-aligned VLS-grown planar nanostructures, Nanoscale, 7, (2015), 20442-20450.
[19] T. Paulauskas, V. Pačebutas, R. Butkutė, B. Čechavičius, A. Naujokaitis, M. Kamarauskas, M. Skapas, J. Devenson, M. Čaplovičová, V. Vretenár, Atomic-resolution EDX, HAADF, and EELS study of GaAs1-xBix alloys, Nanoscale Research Letters, 15, (2020), 1-12.
[20] G. Vardar, S. Paleg, M. Warren, M. Kang, S. Jeon, R. Goldman, Mechanisms of droplet formation and Bi incorporation during molecular beam epitaxy of GaAsBi, Applied Physics Letters, 102, (2013), 042106.
[21] J. Steele, R.A. Lewis, J. Horvat, M.J.B. Nancarrow, M. Henini, D. Fan, Y. Mazur, M. Schmidbauer, M. Ware, S.-Q. Yu, Surface effects of vapour-liquid-solid driven Bi surface droplets formed during molecular-beam-epitaxy of GaAsBi, Scientific reports, 6, (2016), 1-17.
[22] S. Zhu, W. Qiu, H. Wang, T. Lin, P. Chen, X. Wang, Raman spectroscopic determination of hole concentration in undoped GaAsBi, Semiconductor Science and Technology, 34, (2018), 015008.
[23] M. Seong, S. Chun, H.M. Cheong, N. Samarth, A. Mascarenhas, Spectroscopic determination of hole density in the ferromagnetic semiconductor Ga 1− x Mn x As, Physical Review B, 66, (2002), 033202.
[24] J. Steele, R. Lewis, M. Henini, O. Lemine, D. Fan, Y.I. Mazur, V. Dorogan, P. Grant, S.-Q. Yu, G. Salamo, Raman scattering reveals strong LO-phonon-hole-plasmon coupling in nominally undoped GaAsBi: optical determination of carrier concentration, Optics express, 22, (2014), 11680-11689.
[25] D. Schmeltzer, R. Beserman, Localized states in mixed Ga P z As 1− z crystals, Physical Review B, 22, (1980), 6330.
[26] P. Verma, K. Oe, M. Yamada, H. Harima, M. Herms, G. Irmer, Raman studies on Ga As 1− x Bi x and In As 1− x Bi x, Journal of Applied Physics, 89, (2001), 1657-1663.
[27] G. Irmer, M. Wenzel, J. Monecke, Light scattering by a multicomponent plasma coupled with longitudinal-optical phonons: Raman spectra of p-type GaAs: Zn, Physical Review B, 56, (1997), 9524.
[28] D.E. Aspnes, A. Studna, Dielectric functions and optical parameters of si, ge, gap, gaas, gasb, inp, inas, and insb from 1.5 to 6.0 ev, Physical review B, 27, (1983), 985.
[29] J. Blakemore, Semiconducting and other major properties of gallium arsenide, Journal of Applied Physics, 53, (1982), R123-R181.
[30] H. Alghamdi, V.O. Gordo, M. Schmidbauer, J.F. Felix, S. Alhassan, A. Alhassni, G.A. Prando, H. Coelho-Júnior, M. Gunes, H.V.A. Galeti, Effect of thermal annealing on the optical and structural properties of (311) B and (001) GaAsBi/GaAs single quantum wells grown by MBE, Journal of Applied Physics, 127, (2020), 125704.
[31] S. Imhof, C. Wagner, A. Thränhardt, A. Chernikov, M. Koch, N.S. Köster, S. Chatterjee, S.W. Koch, O. Rubel, X. Lu, Luminescence dynamics in ga (asbi), Applied Physics Letters, 98, (2011), 161104.
[32] R. Loudon, The Raman effect in crystals, Advances in Physics, 13, (1964), 423-482.

[33] J. Groenen, G. Landa, R. Carles, P. Pizani, M. Gendry, Tensile and compressive strain relief in In x Ga 1− x As epilayers grown on InP probed by Raman scattering, Journal of applied physics, 82, (1997), 803-809.
[34] P. Wickboldt, E. Anastassakis, R. Sauer, M. Cardona, Raman phonon piezospectroscopy in GaAs: Infrared measurements, Physical Review B, 35, (1987), 1362.
[35] Q. Kim, D. Langer, Effects of excitation intensity on photoluminescence of pure CdTe, physica status solidi (b), 122, (1984), 263-268.
[36] S. Mazzucato, P. Boonpeng, H. Carrère, D. Lagarde, A. Arnoult, G. Lacoste, T. Zhang, A. Balocchi, T. Amand, X. Marie, Reduction of defect density by rapid thermal annealing in GaAsBi studied by time-resolved photoluminescence, Semiconductor science and technology, 28, (2013), 022001.
[37] X. Liu, A. Prasad, J. Nishio, E. Weber, Z. Liliental-Weber, W. Walukiewicz, Native point defects in low-temperature-grown GaAs, Applied Physics Letters, 67, (1995), 279-281.
[38] S. Tixier, M. Adamcyk, T. Tiedje, S. Francoeur, A. Mascarenhas, P. Wei, F. Schiettekatte, Molecular beam epitaxy growth of GaAs 1− x Bi x, Applied physics letters, 82, (2003), 2245-2247.
[39] Y. Liu, X. Yi, N.J. Bailey, Z. Zhou, T.B. Rockett, L.W. Lim, C.H. Tan, R.D. Richards, J.P. David, Valence band engineering of GaAsBi for low noise avalanche photodiodes, Nature communications, 12, (2021), 4784.
[40] G. Nelson, D. Reilly, Gamma-ray interactions with matter, Passive nondestructive analysis of nuclear materials, 2, (1991), 27-42.
[41] C. Weiss, S. Park, J. Lefèvre, B. Boizot, C. Mohr, O. Cavani, S. Picard, R. Kurstjens, T. Niewelt, S. Janz, Electron and proton irradiation effect on the minority carrier lifetime in SiC passivated p-doped Ge wafers for space photovoltaics, Solar Energy Materials and Solar Cells, 209, (2020), 110430.
[42] L. Zhao, M. Konczykowski, H. Deng, I. Korzhovska, M. Begliarbekov, Z. Chen, E. Papalazarou, M. Marsi, L. Perfetti, A. Hruban, Stable topological insulators achieved using high energy electron beams, Nature Communications, 7, (2016), 10957.
[43] S. Aldawood, S. AlGamdi, S.A. Salman, M. AlGarawi, T.S. Alkhuraiji, S.M. Ali, Influence of γ-ray exposure and dose dependent characteristics of (n) PbS–(p) Si hetero-structure, Journal of Materials Science: Materials in Electronics, 32, (2021), 11616-11627.
[44] S. Olsthoorn, F. Driessen, A. Eijkelenboom, L. Giling, Photoluminescence and photoluminescence excitation spectroscopy of Al0. 48In0. 52As, Journal of applied physics, 73, (1993), 7798-7803.
[45] H. Sun, S. Calvez, M. Dawson, J. Gupta, G. Aers, G. Sproule, Thermal quenching mechanism of photoluminescence in 1.55 μ m Ga In N As Sb⁄ Ga (N) As quantum-well structures, Applied physics letters, 89, (2006), 101909.
[46] M. Usman, C.A. Broderick, A. Lindsay, E.P. O'Reilly, Tight-binding analysis of the electronic structure of dilute bismide alloys of GaP and GaAs, Physical Review B, 84, (2011), 245202.
[47] S. Sze, K.K. Ng, LEDs and Lasers, Physics of Semiconductor Devices, 3, (2006), 601-657.